Environmental Nanotechnology, Monitoring & Management 20 (2023) 100892

Contents lists available at ScienceDirect

Environmental Nanotechnology, Monitoring & Management

journal homepage: www.elsevier.com/locate/enmm

Novel one-step synthesis of solid-state carbonized polymer dots by heating at around melting point of polyethylene terephthalate (PET) bottle plastic waste

Mahardika Prasetya Aji [a,*], Ita Rahmawati [b], Aan Priyanto [b], Putut Marwoto [a]

[a] Department of Physics, Universitas Negeri Semarang, Jalan Taman Siswa, Sekaran, Gunungpati Semarang, Central Java 50229, Indonesia
[b] Department of Physics, Faculty of Mathematics and Natural Sciences, Institut Teknologi Bandung, Jalan Ganesha 10, Bandung, West Java 40132, Indonesia

ARTICLE INFO

Keywords:
Carbonized polymer dots
Solid-state fluorescence
Polyethylene terephthalate
Melting point

ABSTRACT

Production of luminescent carbonized polymer dots (CPDs) in the solid state has been a crucial challenge due to their tendency to self-aggregate, leading to fluorescence quenching and limiting their applicability in the solid state. In this work, we present an environmentally friendly method for producing solid-state CPDs with high photoluminescence (PL) intensity by simple one-step heating method using waste PET bottle plastic as the raw material. Based on the PET thermal analysis, heating temperatures between 200 °C and 300 °C and heating duration were explored. Through systematic experimentation, we discovered that heating temperature and time play a crucial role in controlling PL intensity, ultraviolet–visible (UV–Vis) absorption, carbonization degree, and structure of CPDs. The carbonization of CPDs occurs when the heating temperature exceeds the PET melting point, resulting in strong PL characteristics in the range of 400 and 600 nm. However, when the temperature rises, the PL decreases as the number of oxygen-containing functional groups on the surface of CPDs increases. The optimal conditions for high PL intensity were 260 °C for 2.5 h. Our one-step heating approach provides a cost-effective solution for recycling PET waste, offering promising potential for various applications.

1. Introduction

Plastic bottles are commonly encountered packaging materials due to their versatility, durability, and low cost (Benyathiar et al., 2022; Rodríguez-Hernández et al., 2019). It is expected that around 62 % of all plastic bottles have been made from polyethylene terephthalate (PET) (Amirudin et al., 2022; Becerril-Arreola and Bucklin, 2021; Zhang et al., 2020). Nowadays, it is very convenient to use PET bottles as single-use beverage packaging. Consequently, disposable PET bottles accumulate as waste and become a significant environmental concern due to their non-biodegradable properties. The biodegradation of PET waste can take up to 500 years and releases harmful toxins into the water and soil, posing risks to human health and biodiversity (Becerril-Arreola and Bucklin, 2021; Gao et al., 2022; Ghosh and Das, 2021). Incineration is a common method for disposing of PET waste, but it contributes to air pollution and releases high CO_2 emissions that exacerbate greenhouse effects and climate change (Song et al., 2019; Yin et al., 2021). Thus, there is a pressing need for a more environmentally friendly method to increase the value of these waste materials. Recently, alternative methods have been developed to process PET wastes as a promising source for synthesis of carbon-based nanomaterial, such as carbon dots (Ghosh and Das, 2021; Hu et al., 2021, 2019; Johnson et al., 2021; Rodríguez-Hernández et al., 2019).

Carbonized polymer dots (CPDS) belong to the class of carbon dots and have emerged as a very promising group of zero-dimensional carbon-based nanomaterial that have gained significant attention for their outstanding properties, such as chemical stability, low toxicity, and good optical stability, showing promising potential for many advanced applications (Bagheri et al., 2017; Mansuriya and Altintas, 2021; Song et al., 2019). CPDs have a carbon/polymer hybrid structure with a carbon core, abundant surface functional groups and short polymer chains, which are reserved owing to a low or incomplete carbonization degree (Wang et al., 2021; Xia et al., 2019a). Their characteristics and states can be tunable depending on their application (Mansuriya and Altintas, 2021). In recent years, there has been an increased demand for solid-state CPDs in optoelectronic devices, sensors, fingerprint identification, fluorescent ink, security label, and others (Jin et al., 2020; Singaravelu et al., 2021; Wang et al., 2020). However, solid-state CPDs

* Corresponding author.
E-mail address: mahardika@mail.unnes.ac.id (M. Prasetya Aji).

https://doi.org/10.1016/j.enmm.2023.100892
Received 25 June 2023; Received in revised form 19 September 2023; Accepted 26 October 2023
Available online 29 October 2023

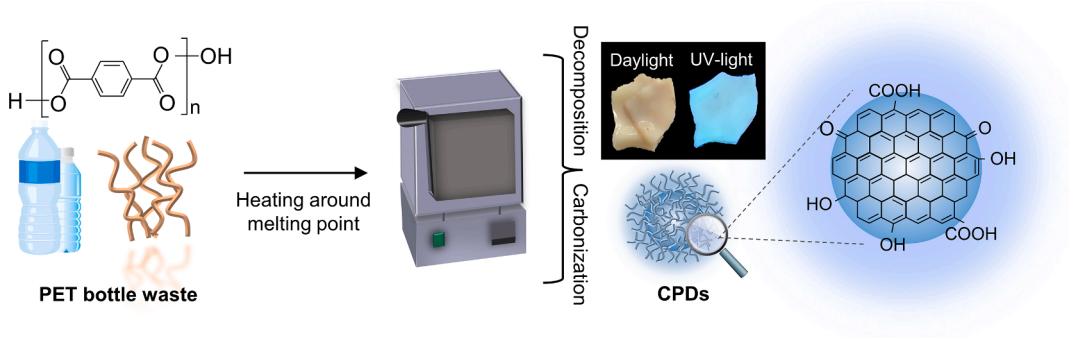

Scheme 1. Mechanism for the preparation of solid-state CPDs based on PET bottle waste.

always suffer from fluorescent quenching due to direct π-π interactions or excessive fluorescence resonance energy transfer (Ren et al., 2021; Singaravelu et al., 2021; Wang et al., 2020), which seriously limits their application in solid-state emissions. Currently, to obtain solid-state fluorescent CPDs, many efforts have been made usually using two main strategies: (i) the synthesis of fluorescent self-quenching-resistant solid-state CPDs, and (ii) blending CPDs with polymers materials to restrict intermolecular motions (Ren et al., 2021; Singaravelu et al., 2021). The second strategy, however, involves a complicated fabrication process and can reduce the optical performance of CPDs (Yoo et al., 2019). Therefore, there is need for the development of solid-state CPDs that are substantially resistant to self-quenching.

Plastic-based CPDs are a great candidate among the various solid-state CPDs since they naturally have hydrophobic qualities, as highlighted by Yin et al (Song et al., 2019). PET plastic-based CPDs, in particular, may also show potential, given their similar properties. Although the final product is liquid-state carbon dots, several studies of PET-based carbon dots have been performed using a two-step synthesis method. Ghosh and Das reported the heating of PET to high temperatures at the first step of synthesis, producing a dark and dry powder resembling carbon black (Ghosh and Das, 2021). Similarly, Hu et al. also conducted a two-step synthesis with the heating of PET at the first step (Hu et al., 2021). However, if the carbonization temperature is optimized, solid-state CPDs with high fluorescent can be yielded without requiring a second synthesis step. As Bagheri and his coworkers reported, the optimum carbonization degree in the synthesis carbon dots was affected by melting point of starting material during heating process. The photoluminescent behavior of carbon dots strongly depends on the temperature of heating during synthesis (Bagheri et al., 2017). To the best of our knowledge, there have been no reports on the investigation of PET-based CPDs in a solid state. Specifically, synthesis according to the thermal decomposition of PET has not been considered.

This study reported a simple synthesis route for producing solid-state CPDs from PET plastic waste. An experiment plan was arranged to

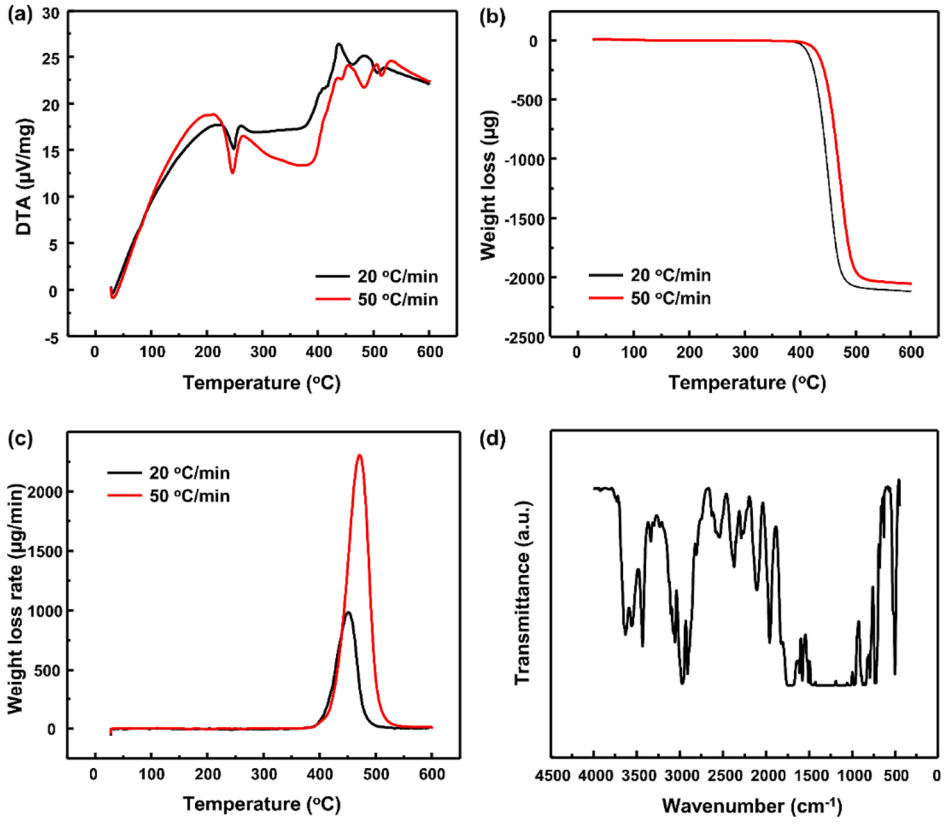

Fig. 1. Starting material (PET bottle waste) analysis: (a) differential thermal analysis (DTA), (b) thermogravimetric analysis (TGA), (c) derivative TGA (DTGA), and (d) Fourier Transform Infrared Spectroscopy (FTIR).

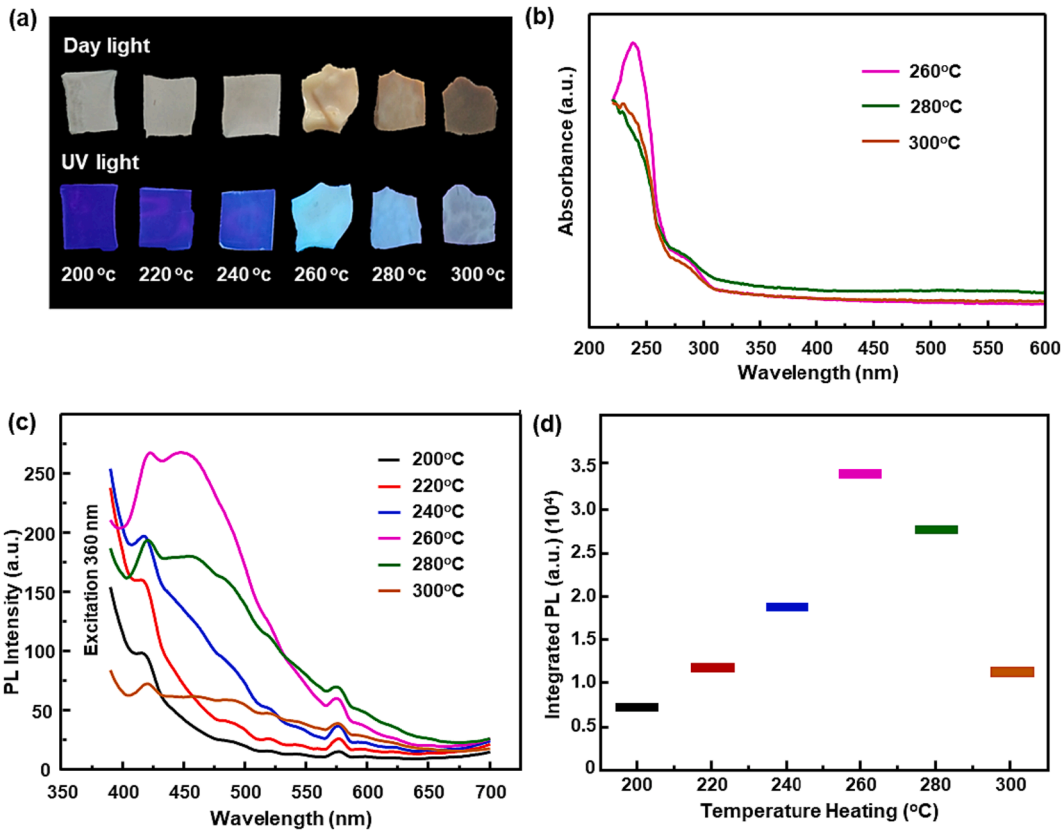

Fig. 2. (a) Solid-state PET-based CPDs under visible light (up) and UV radiation (down) over heating temperature variation, (b) UV–Vis absorption of solid-state PET-based CPDs, (c) PL spectra of the solid-state PET-based CPDs samples under 360 nm, (d) integrated PL of spectra PL from 400 to 650 nm wavelength.

gather the maximum information possible regarding the formation of these materials and the impact of synthesis conditions on their optical and chemical composition. The heating temperatures were investigated around the melting point of PET because carbon chains in the polymer decompose at temperatures above the melting point, which may lead to nucleation processes generating carbon cores. This study opens up a new understanding of the melting temperature as a critical point for synthesizing CPDs which only a few researchers have pointed out. In addition, the synthesis process does not require toxic, corrosive, or expensive solvents which are typically employed in synthesizing CPDs. The production of solid-state fluorescent CPDs from PET plastic waste increases the added value of PET waste and opens opportunities for future research in plastic waste management.

2. Material and methods

2.1. Synthesis of CPDs

The solid-state CPDs were prepared by a one-step heating method using PET bottle waste as a carbon source. First, a waste PET bottle was collected and washed subsequently using water. The dried PET bottle was cut into small flakes and, afterward, transferred in a crucible for air oxidation in a muffle furnace at various temperatures ranging from 200 °C to 300 °C for 2.5 h. The optimal temperature was determined to be 240 °C and was selected for the heating durations of 1 h to 3 h. The resulting solid-state product was collected and then characterized.

2.2. Characterization

UV–visible absorption spectra were recorded using a BMG Labtech Fluostar Omega spectrometer. Fluorescence measurements were carried out using a Cary Eclipse MY14440002 spectrofluorometer. Integrated fluorescence intensity is the area under the PL curve in the wavelength range from 400 to 650 nm. Fourier Transform Infrared (FTIR) spectra were recorded for powder CPDs using the Perkin-Elmer Spectrum Version 10.03.06 with an ATR attachment. Thermogravimetric analysis (TGA) was performed using a STA7300 Hitachi with a heating rate of 20 °C/min and 50 °C/min. Raman spectroscopy was measured using Horiba LabRAM HR Evolution Laser 785 nm. XRD measurements were performed using a Rigaku Smart Lab X-Ray diffractometer with CuK α radiation at a wavelength of $\lambda = 1.540\dot{A}$ to determine the crystalline phase of the synthesized samples. The size of the CPDs were investigated using TEM measurements performed on a HT7700 Hitachi at 80 kV.

3. Results and discussion

The solid-state CPDs were synthesized from PET bottle waste using a simple heating process in a muffle furnace without any additional chemicals (Scheme 1). In preparing CPDs using the heating method, the PET chains were decomposed, followed by carbonization and then solid-state CPDs were formed. In this study, a systematic synthesis study was conducted by setting the synthesis temperature at around the melting point of PET and varying the heating duration to get the maximum information possible. The DTA of PET bottle waste (Fig. 1a) showed a strong endothermic peak at around 250 °C, implying a melting point of PET. Melting occurs when atomic vibrations are vigorous enough to rupture large numbers of atomic bonds in PET. For polymers, upon cooling through the melting temperature, nuclei form wherein small regions of the tangled and random molecules become ordered and aligned. At temperatures in excess of the melting temperature, these nuclei are unstable due to the thermal atomic vibrations that tend to disrupt the ordered molecular arrangements. After nucleation and during the growth stage, nuclei grow through the continued ordering and alignment of additional molecular chain segments (Callister, 2001). On

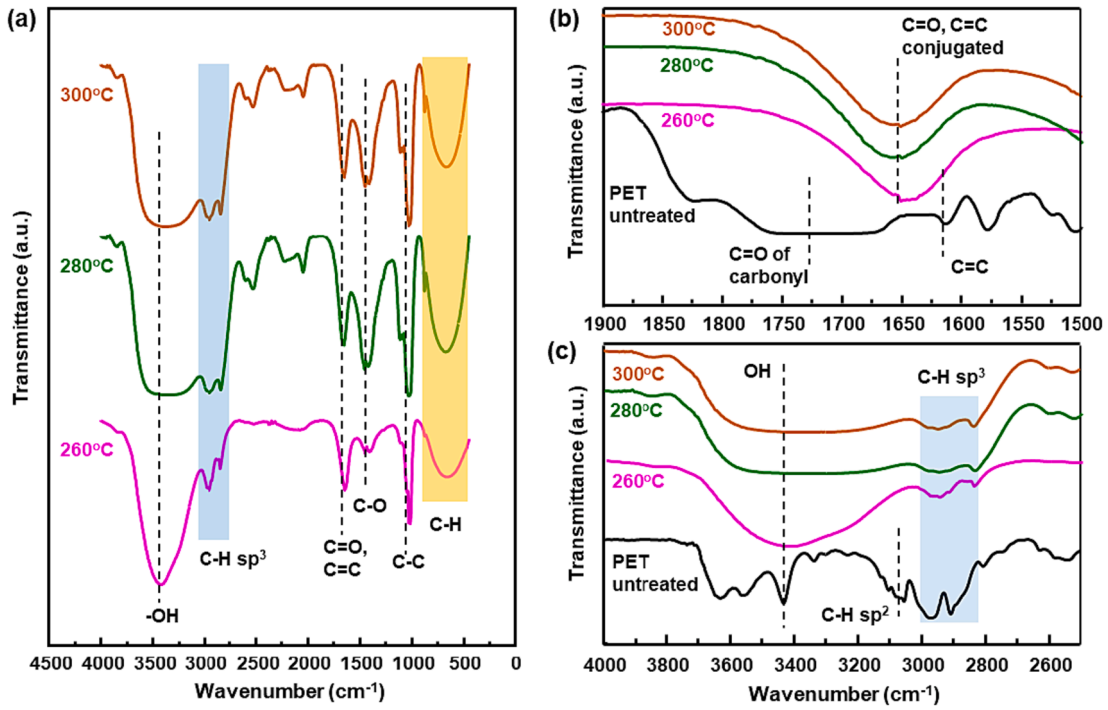

Fig. 3. (a) FTIR spectra of PET-CPDs with different temperature heating at full region, (b) FTIR spectra at C=C and C=O region of PET-CPDs with different temperature heating compared with untreated PET, and (c) FTIR spectra at OH, C-H sp^2 and C-H sp^3 region of PET-CPDs with different temperature heating compared with untreated PET.

the other hand, the TGA curve (Fig. 1b and c) confirmed a decrease in weight loss, with the thermal degradation of PET onsets at 380 °C (at heating rate 20 °C/min) and at 395 °C (at heating rate 50 °C/min). The results also reveal that the heating rate affects the DTA and TGA test results, however the difference is not significant.

Furthermore, FTIR analysis shows that PET plastic bottles (Fig. 2d) showed the presence of broad molecular groups consisting of carbon, hydrogen, and oxygen. The C-H stretching vibration modes appear in the region 3000–2825 cm^{-1} that refer to the functional groups such as alkyl, alkanal, alkyne, alkene, and arene. The C-H bending mode of vibration, which has weaker bond strength than their stretching modes, appears in the region 924–808 cm^{-1} and 573 cm^{-1} (Prasad et al., 2011). The absorption at 3412 cm^{-1} is assigned to the O-H stretching at the end group of the PET molecule chain. The C=O stretching and the aromatic skeleton stretching bands were observed at 1730 and 1614 cm^{-1}, respectively (Torres-Huerta et al., 2016).

The distribution of the samples with different heating temperatures is shown in Fig. 2a. Physically, the samples heated at temperatures ranging from 200 to 240 °C (below the melting point) remained transparent but exhibited increased brittleness and shrinkage compared to the unheated sample. On the other hand, the samples heated over the melting point (260–300 °C) showed significant physical alteration, such as becoming opaque, extremely brittle, and undergoing a color from light brown to dark brown. Moreover, under UV light, the results revealed that samples heated between 200 and 240 °C exhibited no luminescence. Meanwhile, samples of 260–300 °C showed luminescence, with samples of 260 °C having the brightest luminescence. This result indicated that determining the synthesis temperature around the melting point is one of the most crucial variables in producing CPDs with excellent luminescence.

The UV–Vis absorption spectra of the samples with varying synthesis temperatures are depicted in Fig. 2b. Samples at 200–240 °C were not characterized due to their high stickiness and very weak luminescence. The UV–Vis spectra displayed absorption in the UV region of 220–300 nm. A stronger peak was observed at 240 nm with a shoulder at 280 nm originating from π-π^* transition of C-C and C=C in aromatic rings of the carbon core and n-π^* transition of oxygen-related bonds (C=O and C–O) on the surface state of CPDs, respectively (Ding et al., 2016; Y. Y. Liu et al., 2021). In the case of the 260 °C sample (CPDs-260), the peak at 240 nm was higher than in the other CPDs, indicating that it has stronger absorption properties. This result supports the conclusion that the synthesis temperature has a significant effect on the absorption properties of the synthesized CPDs (Zhang et al., 2016).

The PL spectra of the as-synthesized CPDs at different temperatures are depicted in Fig. 2c. Upon excitation at 360 nm, PL intensity also shows a similar trend as the 240 nm peak of CPDs absorption intensity, suggesting the luminescence of solid-state PET-based CPDs may originate from the π-π* bond transition in the carbon core. Widely proposed luminescence mechanisms of CPDs originate from the conjugated π-domain within the graphitic carbon core, the surface state, or the molecular state of CPDs (Ai et al., 2021; Xia et al., 2019b). Here, the emission of PET-based CPDs belonged to the core-state luminescence mechanism category. Under 360 nm irradiation, the luminescence of solid-state CPDs centered at 450 nm, indicating blue color (in line with the physical appearance Fig. 2a). Additionally, it is apparent that the photoluminescence (PL) spectrum has a little peak at a wavelength of 575 nm. The observed peak suggests that PET-CPDs exhibit multiple emission centers, with the additional emission usually due to the presence of polycyclic aromatic hydrocarbons of varying sizes. This is in comparison with the conjugated sp^2 domains formed during the dehydration of the polymeric structure (Shamsipur et al., 2018).

As shown in Fig. 2d, the integrated fluorescence intensity is derived from the area under the PL curve in the 400 to 650 nm range. The PL intensity changes with heating temperature, and CPDs-260 has the highest intensity. However, the PET-based CPDs emit less light and look black when the heating temperature is quite higher than the melting point, indicating that carbonization occurs during the formation of CPDs. Due to the severe aggregation-caused quenching, most CPDs show no fluorescence in the solid state (B. Liu et al., 2021). This study obtained solid-state PET-CPDs with strong blue photoluminescence without aggregation. The observed phenomenon can be attributed to the presence of a large number of surface PET chains surrounding the core of

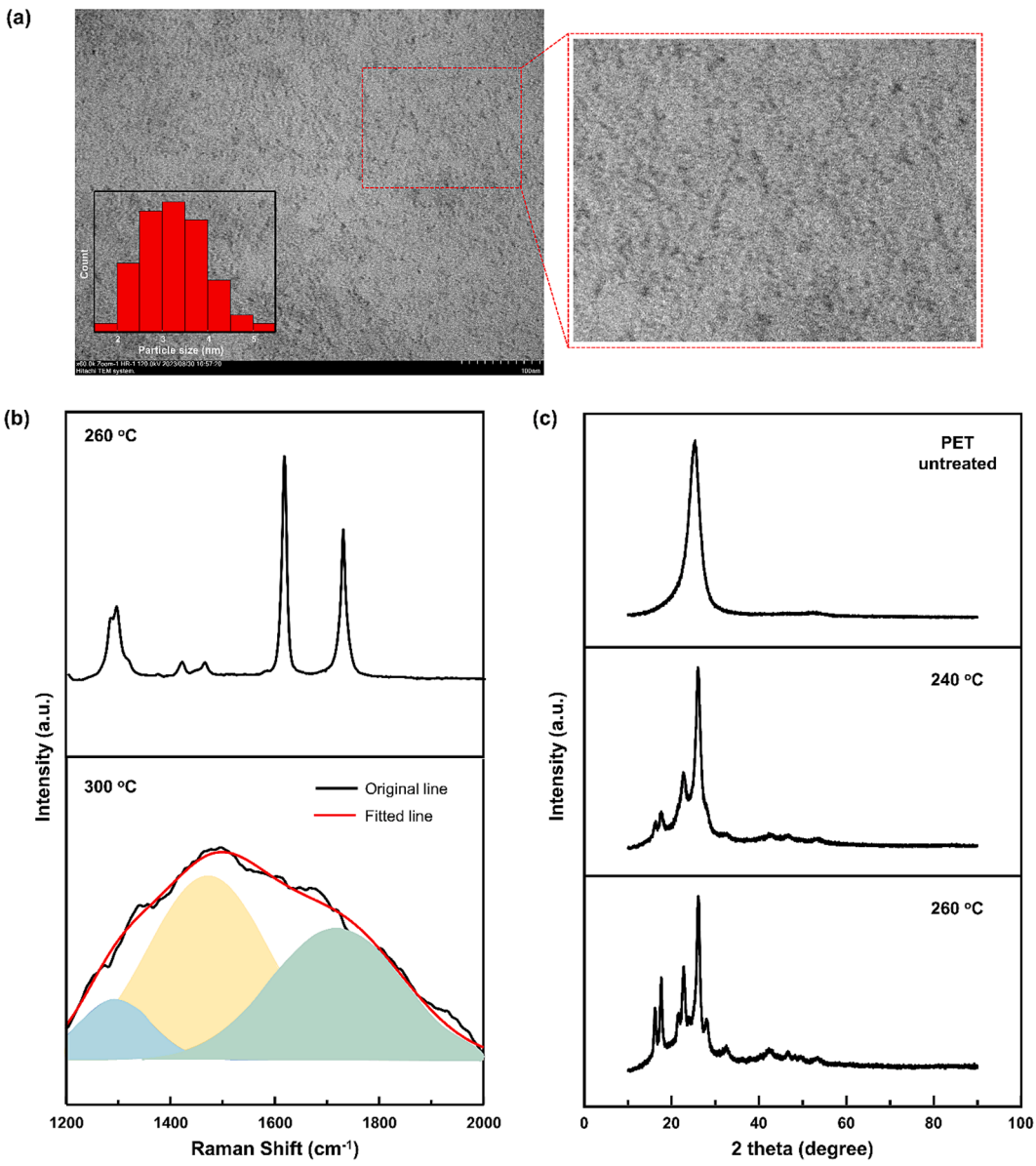

Fig. 4. (a) TEM of PET-CPDs by heating at 260 °C (b) Raman shifts of PET-CPDs by heating at 260 °C and 300 °C, and (c) XRD of PET and PET-CPDs by heating at 240 °C and 260 °C.

CPDs, which effectively prevents π-π interactions. Consequently, the quenching process induced by aggregation is blocked. In addition, it is worth noting that PET-CPDs exhibit strong hydrophobic characteristics, in contrast to many other CPDs that possess hydrophilic surfaces. This characteristic limits the electrostatic interaction and particle attraction of CPDs (Ru et al., 2022; Yang et al., 2019).

As shown in Fig. 3, Fourier Transform Infrared (FTIR) was performed to determine the composition of the PET-CPDs. The FTIR results confirmed the presence of different functional groups in the synthesized CPDs, including oxygen, hydrogen, and carbon (Fig. 3a). Compared to the FTIR results of untreated PET, some of the PET composition significantly changed after heating above the melting point, indicating decomposition occurred during the heating process (Fig. 3a). The absorbance at 1430 cm^{-1} changed significantly, indicating a C-O group presence. The higher the temperature, the more energy the sample will attach to ambient oxygen. In addition, changes at 1670 cm^{-1} were observed, indicating conjugated C=C and C=O bonds (Fig. 3b). The untreated PET showed a C=C bond from the aromatic skeleton at 1610 cm^{-1} and the C=O bond from the carbonyl at 1720 cm^{-1}. However, when the PET was heated above the melting point, the C=C and C=O frequencies shifted and were no longer distinguishable, moving to 1660 cm^{-1} and indicating conjugation of the carbonyl group with a C=C double bond. The presence of the C=C and C=O bond signatures suggests forming a π-conjugated system as CPDs core structure (Permatasari et al., 2021). This conjugation bond plays a role in the CPDs photoluminescence process, which is related to the energy gap (Permatasari et al., 2021; Semeniuk et al., 2019; Wang et al., 2017). The results of this study demonstrate that temperatures above the melting point can lead to the formation of conjugate bonds in the aromatic skeleton of the PET-based CPDs, resulting in solid luminescence. However, CPDs-280 and CPDs-300 have lower luminescence intensity (as previously demonstrated in Fig. 2c) due to a large number of attached oxygen bonds. These oxygen-containing groups lead to non-radiative coupling of electron-hole pairs that suppress CPDs PL (Ai et al., 2021). In addition, as depicted in Fig. 3c, PET-CPDs feature C-H sp^3 bond vibrations between 3000 and 2800 cm^{-1}, suggesting the carbon core of the PET-CPDs. In contrast, untreated PET possessed C-H sp^2 bonds that vanished upon heating, indicating that heating at temperatures above the melting point

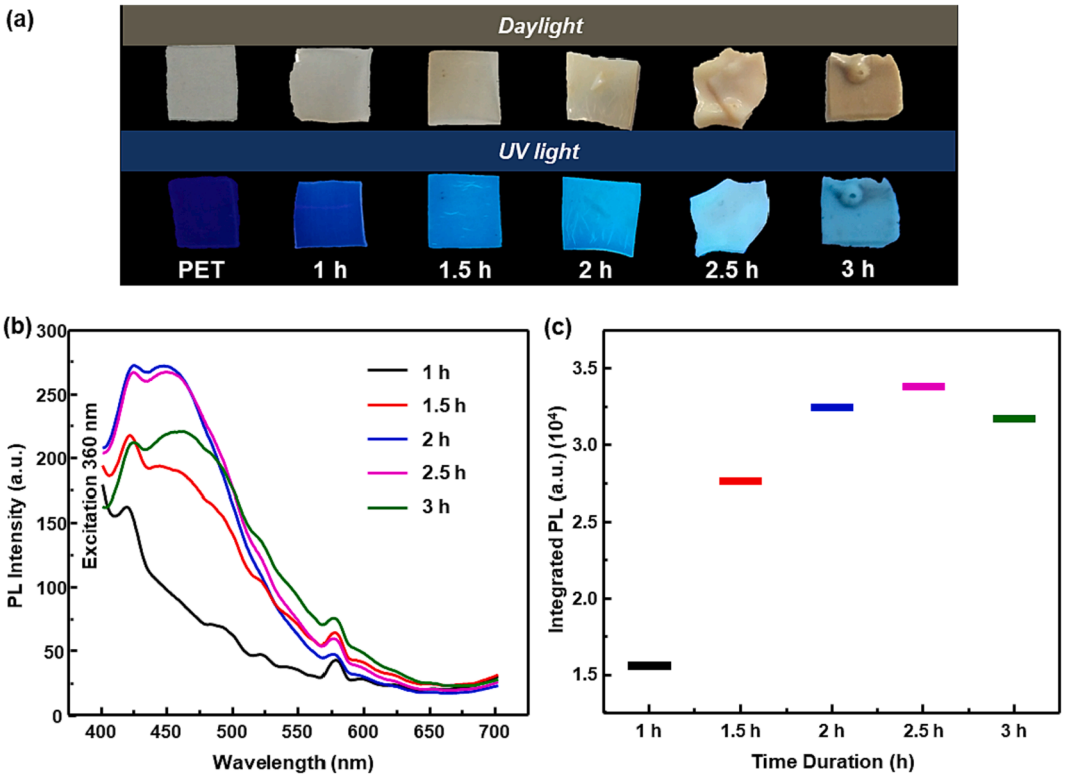

Fig. 5. Dependence of the photoluminescence (PL) properties of CPDs on heating time: a) physical appearance emission of PET-CPDs, (b) PL spectra of PET-CPDs, and (c) integrated PL as a function of time duration of hearing and PL intensity.

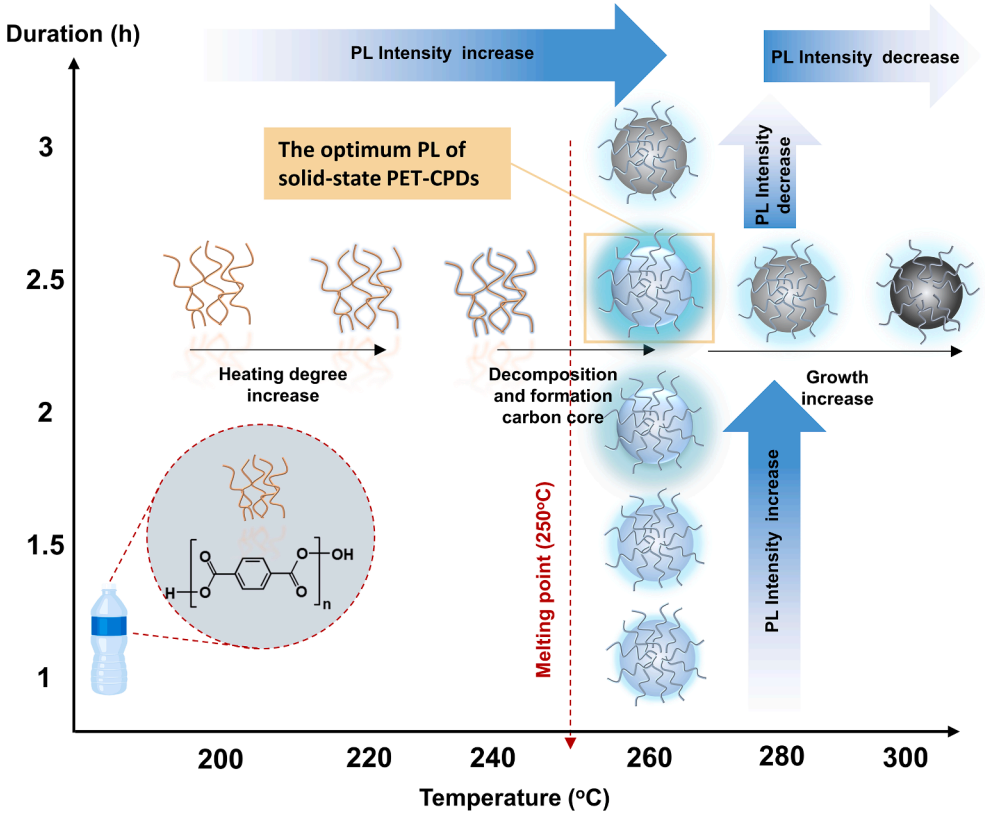

Fig. 6. Schematic representation of the emission characteristics of PET-CPDs over temperature and time scales and schematic possibility of mechanism of CPDs formation.

Table 1
Comparison of various reported CPDs material from PET.

No	Synthetic method	Reaction condition	Product	Average size	Emission	Ref.
	Microwave reactor – hydrothermal method	260 °C, 24 h	Solution	2.8 nm	Green	(Wu et al., 2022)
	Two-step approach (carbonization followed by hydrothermal treatment)	muffle furnace at 350 °C for 2 h, autoclave at 170 °C for 8 h	Solution	6 nm	Blue	(Ghosh and Das, 2021)
	Heating – hydrothermal method	Heated at 350 °C for 2 h, Hydrothermal 180 °C for 12 h	Solution	6 nm	Blue	(Hu et al., 2019)
	Air oxidation	300 °C for 2 h then immerse in H_2SO_4 at 120 °C for 6 h	Solution	3 nm	–	(Hu et al., 2021)
	Quenched into liquid nitrogen	–	Yellowish paste	2.3 nm	Blue	(Yin et al., 2021)
	Heating treatment	260 °C, 2 h	Solid	3.27 nm	Blue	This work

decomposed the original PET structure.

The morphology and size distribution of PET-based CPDs obtained under optimal conditions were explored by TEM. As displayed in Fig. 4a, PET-based CPDs s are spherical in shape, uniform, and well distributed without aggregation. The particle size distribution histogram represented in the inset of Fig. 2b disclosed their homogeneous size distribution of 1 – 6 nm and average diameter of 3.28 ± 0.74 nm. The structural characteristics of the PET-CPDs were further analyzed using Raman scattering, as shown in Fig. 4a. The PET-based CPDs at 260 °C exhibit a Raman peak at 1300 cm^{-1}, corresponding to the vibration of aromatic in-plane CH deformation (Xu et al., 2020). There were also peaks at 1620 and 1760 cm^{-1}, attributed to the ring C-C stretching and C=O stretching, respectively (Aoyama et al., 2014). A peak at ~ 1300 cm^{-1} is often referred to as a peak from the out-of-plane vibrations of sp^2 carbon atoms in the presence of disordered states corresponding to topological sp^3 molecular defect states, while the peak at ~ 1620 cm^{-1} results from the in-plane stretching vibrations of sp^2 carbon atoms within aromatic domain (Bhattacharyya et al., 2017). However, at higher temperatures (300 °C), the spectral peak broadened, indicating that the structure of CPDs became amorphous. This result implies, based on the emission spectra, that the structure of the CPDs also affects the intensity of the generated emissions. Crystalline structures are expected to emit more optimally than amorphous structures due to reduced phonon (non-radiative) scattering losses (Pal et al., 2018).

The XRD pattern of the synthesized PET-based CPDs is shown in Fig. 4c. For comparison, the XRD pattern of untreated PET was also recorded. The XRD of the PET before and after treatment show a noticeable change. The raw PET shows the characteristic peak at $2\theta = 25.5^{o}$ corresponding to the (1 0 0) plane for a semicrystalline PET. After heat treatment, there is also new peaks at 17.5° and 22.5° corresponding to the (1 1 0) and (0 1 0) planes, respectively. The observed peak at a 2θ of 22.5° can be attributed to the increased presence of the amorphous region in contrast to the crystalline region (Agrawal et al., 2018). This observation implies that the heating treatment has an impact on the surface of PET.

The role of reaction time on the properties of the materials is displayed in Fig. 5. Again, the emission of the PET-based CPDs strongly depends on the reaction time as well. The physical appearance of PET-based CPDs (Fig. 5a) indicates that the sample is photoluminescent after being heated for more than 1 h at a heating temperature over the melting point (260 °C). Optimal emission is observed in PET-based CPDs heated for 2.5 h, as demonstrated by the photoluminescence spectra shown in Fig. 5b. Modifying the heating time results in a shift in the emission peak of the PET-based CPDs to 450 nm, similar to the variation observed with heating temperature. As illustrated in Fig. 5c, the highest intensity of the PET-based CPDs was observed at 2.5 h of heating, followed by a decrease in intensity after heating for 3 h.

Fig. 6 summarizes our findings. The schematic correlates the PL intensity of the PET-CPDs obtained during different stages of heating, which is primarily attributed to the conjugation of the aromatic core. As the temperature increases, the number of oxygen-containing groups grows and contributes to the suppressed emission of the aromatic core. The optimal PL intensity is observed in PET-based CPDs at 260 °C with a 2.5 h heating duration. Initially, the polymer of PET is non-fluorescent molecules. However, under low heating temperatures (below its melting point), the PET bonds do not decompose but become more wrinkled. When the degree of heating is increased above the melting point (260 °C), the PET carbon chain linkages decompose and carbonize, forming carbon core CPDs with a conjugated aromatic core structure. This conjugation determines the photoluminescence properties of the CPDs. At higher temperatures (from 280 °C to 300 °C), the carbon core gradually grows, and the number of oxygen-containing groups on the surface of PET-based CPDs increases, leading to a decrease in the intensity of CPDs. The duration of heating also has a significant impact on the intensity of PET-based CPDs obtained. The carbon chain bonds decompose by heating PET above its melting point (260 °C), but sufficient heating time is necessary to generate an appropriate carbon core with conjugated bonds. In this study, the optimal duration was 2.5 h. In conclusion, the PL intensity of PET-based CPDs is influenced by the number of oxygen-containing groups and the growth of the carbon core so that the PET-based CPDs with the highest intensity PL is obtained at appropriate heating temperature and duration.

In comparison to CPDs material derived from PET that has been previously reported, our CPDs exhibit comparable results to most reports (Table 1). It is worth mentioning that some reports showed a more complicated and expensive synthesis process, suggesting our PET-CPDs provide better economic value. Additionally, the mass product yield of the PET-CPDs in a single manufacturing process is 0.028 g. Due to the relatively low temperature employed (slightly higher than the melting point and significantly lower than the weight loss temperature), the utilized method has great potential for large-scale production of CPDs.

4. Conclusions

In summary, we have demonstrated a one-step synthetic route to convert PET bottle waste into solid-state fluorescent CPDs. The PL properties of the solid-state PET-CPDs prepared by a heating method strongly depend on the temperature and duration. This study used the thermal decomposition (melting point) of PET to determine the synthesis temperature and could study the effect of that temperature on the PL properties of PET-based CPDs. We discovered that PET-based CPDs fabricated at 260 °C for 2.5 h exhibit the highest fluorescence intensity. The results indicate that the melting point of PET plays a crucial role the in formation of conjugation aromatic core of CPDs. The carbonization degree would increase not only at longer heating durations, but also as a result of higher heating temperatures after melting point. These findings offer a promising solution for plastic waste management and a simple, green synthesis route for the production of solid-state fluorescent CPDs without the problem of self-quenching.

CRediT authorship contribution statement

Mahardika Prasetya Aji: Conceptualization, Supervision, Data curation, Formal analysis, Resources, Validation, Writing – review & editing. **Ita Rahmawati:** Conceptualization, Methodology, Investigation, Formal analysis, Visualization, Writing – original draft, Writing – review & editing. **Aan Priyanto:** Visualization, Formal analysis, Investigation, Validation, Writing – review & editing. **Putut Marwoto:** Supervision, Visualization, Data curation, Formal analysis, Validation, Writing – review & editing.

Declaration of Competing Interest

The authors declare that they have no known competing financial interests or personal relationships that could have appeared to influence the work reported in this paper.

Data availability

Data will be made available on request.

References

Agrawal, S., Ingle, N., Maity, U., Jasra, R.V., Munshi, P., 2018. Effect of Aqueous HCl with Dissolved Chlorine on Certain Corrosion-Resistant Polymers. ACS Omega 3, 6692–6702. https://doi.org/10.1021/acsomega.8b00515.

Ai, L., Yang, Y., Wang, B., Chang, J., Tang, Z., Yang, B., Lu, S., 2021. Insights into photoluminescence mechanisms of carbon dots: advances and perspectives. Sci. Bull. 66, 839–856. https://doi.org/10.1016/j.scib.2020.12.015.

Amirudin, A., Inoue, C., Grause, G., 2022. Analyzing Polyethylene Terephthalate Bottle Waste Technology Using an Analytic Hierarchy Process for Developing Countries: A Case Study from Indonesia. Recycling 7. https://doi.org/10.3390/recycling7040058.

Aoyama, S., Park, Y.T., Ougizawa, T., Macosko, C.W., 2014. Melt crystallization of poly (ethylene terephthalate): Comparing addition of graphene vs. carbon nanotubes. Polymer (Guildf.) 55, 2077–2085. https://doi.org/10.1016/j.polymer.2014.02.055.

Bagheri, Z., Ehtesabi, H., Rahmandoust, M., Ahadian, M.M., Hallaji, Z., Eskandari, F., Jokar, E., 2017. New insight into the concept of carbonization degree in synthesis of carbon dots to achieve facile smartphone based sensing platform. Sci. Rep. 7, 1–11. https://doi.org/10.1038/s41598-017-11572-8.

Becerril-Arreola, R., Bucklin, R.E., 2021. Beverage bottle capacity, packaging efficiency, and the potential for plastic waste reduction. Sci. Rep. 11, 1–11. https://doi.org/10.1038/s41598-021-82983-x.

Benyathiar, P., Kumar, P., Carpenter, G., Brace, J., Mishra, D.K., 2022. Polyethylene Terephthalate (PET) Bottle-to-Bottle Recycling for the Beverage Industry: A Review. Polymers (Basel) 14. https://doi.org/10.3390/polym14122366.

Bhattacharyya, S., Ehrat, F., Urban, P., Teves, R., Wyrwich, R., Döblinger, M., Feldmann, J., Urban, A.S., Stolarczyk, J.K., 2017. Effect of nitrogen atom positioning on the trade-off between emissive and photocatalytic properties of carbon dots. Nat. Commun. 8, 1–9. https://doi.org/10.1038/s41467-017-01463-x.

Callister, W.D., 2001. Fundamentals of Materials Science and Engineering.

Ding, H., Yu, S.B., Wei, J.S., Xiong, H.M., 2016. Full-color light-emitting carbon dots with a surface-state-controlled luminescence mechanism. ACS Nano 10, 484–491. https://doi.org/10.1021/acsnano.5b05406.

Gao, Z., Ma, B., Chen, S., Tian, J., Zhao, C., 2022. Converting waste PET plastics into automobile fuels and antifreeze components. Nat. Commun. 13, 1–9. https://doi.org/10.1038/s41467-022-31078-w.

Ghosh, A., Das, G., 2021. Environmentally benign synthesis of fluorescent carbon nanodots using waste PET bottles: Highly selective and sensitive detection of Pb2+ ions in aqueous medium. New J. Chem. 45, 8747–8754. https://doi.org/10.1039/d1nj00961c.

Hu, Y., Gao, Z., Yang, J., Chen, H., Han, L., 2019. Environmentally benign conversion of waste polyethylene terephthalate to fluorescent carbon dots for "on-off-on" sensing of ferric and pyrophosphate ions. J. Colloid Interface Sci. 538, 481–488. https://doi.org/10.1016/j.jcis.2018.12.016.

Hu, Y., Li, M., Gao, Z., Wang, L., Zhang, J., 2021. Waste Polyethylene terephthalate Derived Carbon Dots for Separable Production of 5-Hydroxymethylfurfural at Low Temperature. Catal. Lett. 151, 2436–2444. https://doi.org/10.1007/s10562-020-03484-6.

Jin, K., Zhang, J., Tian, W., Ji, X., Yu, J., Zhang, Jun 2020. Facile access to solid-state carbon dots with high luminescence efficiency and excellent formability via cellulose derivative coatings. ACS Sustain. Chem. Eng. 8, 5937–5945. https://doi.org/10.1021/acssuschemeng.0c00237.

Johnson, L.M., Mecham, J.B., Krovi, S.A., Moreno Caffaro, M.M., Aravamudhan, S., Kovach, A.L., Fennell, T.R., Mortensen, N.P., 2021. Fabrication of polyethylene terephthalate (PET) nanoparticles with fluorescent tracers for studies in mammalian cells. Nanoscale Adv. 3, 339–346. https://doi.org/10.1039/d0na00888e.

Liu, B., Chu, B., Wang, Y.-L., Hu, L.-F., Hu, S., Zhang, X.-H., 2021a. Carbon dioxide derived carbonized polymer dots for multicolor light-emitting diodes. Green Chem. 23, 422–429. https://doi.org/10.1039/D0GC03333B.

Liu, Y.Y., Yu, N.Y., Fang, W.D., Tan, Q.G., Ji, R., Yang, L.Y., Wei, S., Zhang, X.W., Miao, A.J., 2021b. Photodegradation of carbon dots cause cytotoxicity. Nat. Commun. 12, 1–12. https://doi.org/10.1038/s41467-021-21080-z.

Mansuriya, B.D., Altintas, Z., 2021. Carbon Dots: Classification, Properties, Synthesis, Characterization, and Applications in Health Care-An Updated Review (2018-2021). Nanomater. (Basel, Switzerland) 11. https://doi.org/10.3390/nano11102525.

Pal, A., Natu, G., Ahmad, K., Chattopadhyay, A., 2018. Phosphorus induced crystallinity in carbon dots for solar light assisted seawater desalination. J. Mater. Chem. A 6, 4111–4118. https://doi.org/10.1039/C7TA10224K.

Permatasari, F.A., Nakul, F., Mayangsari, T.R., Aimon, A.H., Nuryadin, B.W., Bisri, S.Z., Ogi, T., Iskandar, F., 2021. Solid-state nitrogen-doped carbon nanoparticles with tunable emission prepared by a microwave-assisted method. RSC Adv. 11, 39917–39923. https://doi.org/10.1039/d1ra07290k.

Prasad, S.G., De, A., De, U., 2011. Structural and Optical Investigations of Radiation Damage in Transparent PET Polymer Films. Int. J. Spectrosc. 2011, 1–7. https://doi.org/10.1155/2011/810936.

Ren, J., Stagi, L., Innocenzi, P., 2021. Fluorescent carbon dots in solid-state: From nanostructures to functional devices. Prog. Solid State Chem. 62, 100295 https://doi.org/10.1016/j.progsolidstchem.2020.100295.

Rodríguez-Hernández, A.G., Muñoz-Tabares, J.A., Aguilar-Guzmán, J.C., Vazquez-Duhalt, R., 2019. A novel and simple method for polyethylene terephthalate (PET) nanoparticle production. Environ. Sci. Nano 6, 2031–2036. https://doi.org/10.1039/c9en00365g.

Ru, Y., Waterhouse, G.I.N., Lu, S., 2022. Aggregation in carbon dots. Aggregate 3, 1–14. https://doi.org/10.1002/agt2.296.

Semeniuk, M., Yi, Z., Poursorkhabi, V., Tjong, J., Jaffer, S., Lu, Z.H., Sain, M., 2019. Future perspectives and review on organic carbon dots in electronic applications. ACS Nano 13, 6224–6255. https://doi.org/10.1021/acsnano.9b00688.

Shamsipur, M., Barati, A., Taherpour, A.A., Jamshidi, M., 2018. Resolving the multiple emission centers in carbon dots: from fluorophore molecular states to aromatic domain states and carbon-core states. J. Phys. Chem. Lett. 9, 4189–4198. https://doi.org/10.1021/acs.jpclett.8b02043.

Singaravelu, C.M., Deschanels, X., Rey, C., Causse, J., 2021. Solid-State Fluorescent Carbon Dots for Fluorimetric Sensing of Hg2+. ACS Appl. Nano Mater. 4, 6386–6397. https://doi.org/10.1021/acsanm.1c01400.

Song, H., Liu, X., Wang, B., Tang, Z., Lu, S., 2019. High production-yield solid-state carbon dots with tunable photoluminescence for white/multi-color light-emitting diodes. Sci. Bull. 64, 1788–1794. https://doi.org/10.1016/j.scib.2019.10.006.

Torres-Huerta, A.M., Del Angel-López, D., Domínguez-Crespo, M.A., Palma-Ramírez, D., Perales-Castro, M.E., Flores-Vela, A., 2016. Morphological and mechanical properties dependence of PLA amount in PET matrix processed by single-screw extrusion. Polym. - Plast. Technol. Eng. 55, 672–683. https://doi.org/10.1080/03602559.2015.1132433.

Wang, R., Gu, W., Liu, Z., Liu, Y., Ma, G., Wei, J., 2021. Simple and Green Synthesis of Carbonized Polymer dots from Nylon 66 Waste Fibers and its Potential Application. https://doi.org/10.1021/acsomega.1c04808.

Wang, R., Lu, K.Q., Tang, Z.R., Xu, Y.J., 2017. Recent progress in carbon quantum dots: synthesis, properties and applications in photocatalysis. J. Mater. Chem. A 5, 3717–3734. https://doi.org/10.1039/c6ta08660h.

Wang, J., Yang, Y., Liu, X., 2020. Solid-state fluorescent carbon dots: Quenching resistance strategies, high quantum efficiency control, multicolor tuning, and applications. Mater. Adv. 1, 3122–3142. https://doi.org/10.1039/d0ma00632g.

Wu, Y., Ma, G., Zhang, A., Gu, W., Wei, J., Wang, R., 2022. Preparation of Carbon Dots with Ultrahigh Fluorescence Quantum Yield Based on PET Waste. https://doi.org/10.1021/acsomega.2c05324.

Xia, C., Zhu, S., Feng, T., Yang, M., Yang, B., 2019b. Evolution and Synthesis of Carbon Dots : From Carbon Dots to Carbonized Polymer Dots 1901316. https://doi.org/10.1002/advs.201901316.

Xia, C., Zhu, S., Feng, T., Yang, M., Yang, B., 2019. Evolution and Synthesis of Carbon Dots: From Carbon Dots to Carbonized Polymer Dots. Adv. Sci. https://doi.org/10.1002/advs.201901316.

Xu, G., Cheng, H., Jones, R., Feng, Y., Gong, K., Li, K., Fang, X., Tahir, M.A., Valev, V.K., Zhang, L., 2020. Surface-Enhanced Raman Spectroscopy Facilitates the Detection of Microplastics <1 μm in the Environment. Environ. Sci. Tech. 54, 15594–15603. https://doi.org/10.1021/acs.est.0c02317.

Yang, H., Liu, Y., Guo, Z., Lei, B., Zhuang, J., Zhang, X., Liu, Z., Hu, C., 2019. Hydrophobic carbon dots with blue dispersed emission and red aggregation-induced emission. Nat. Commun. 10, 1–11. https://doi.org/10.1038/s41467-019-09830-6.

Yin, S., Duvigneau, J., Vancso, G.J., 2021. Fluorescent Polyethylene by In Situ Facile Synthesis of Carbon Quantum Dots Facilitated by Silica Nanoparticle Agglomerates. ACS Appl. Polym. Mater. https://doi.org/10.1021/ACSAPM.1C00821.

Yoo, H.J., Kwak, B.E., Kim, D.H., 2019. Self-Quenching Origin of Carbon Dots and the Guideline for Their Solid-State Luminescence. J. Phys. Chem. C 123, 27124–27131. https://doi.org/10.1021/acs.jpcc.9b06154.

Zhang, R., Ma, X., Shen, X., Zhai, Y., Zhang, T., Ji, C., Hong, J., 2020. PET bottles recycling in China: An LCA coupled with LCC case study of blanket production made of waste PET bottles. J. Environ. Manage. 260, 110062 https://doi.org/10.1016/j.jenvman.2019.110062.

Zhang, Y., Wang, Y., Feng, X., Zhang, F., Yang, Y., Liu, X., 2016. Effect of reaction temperature on structure and fluorescence properties of nitrogen-doped carbon dots. Appl. Surf. Sci. 387, 1236–1246. https://doi.org/10.1016/j.apsusc.2016.07.048.